

Supplemental Figures

Figure S1. Eye resection controls and semi-automated eye progenitor counting procedure and results. Related to Figures 1 and 2.

Figure S2. Additional single eye resection BrdU incorporation experiments. Related to Figure 3.

Figure S3. Cell loss controls and combined TUNEL and FISH for *opsin*. Related to Figure 4.

Figure S4. Dynamics of eye growth and de-growth are consistent with a passive model for tissue-specific eye regeneration. Related to Figures 4 and 5.

Figure S5. Eye-resected animals regenerate eyes more slowly than decapitated animals. Related to Figure 5.

Figure S6. Eye progenitor amplification is associated with wounds that induce proliferation in the location of eye progenitor specification. Related to Figures 6 and 7.

Figure S7. Increased progenitor incorporation into the ventral nerve cords and pharynx does not require specific tissue removal. Related to Figure 7.

Supplemental Tables

Table S1. Animal numbers for all experiments. Related to all figures.

Table S2. Sequences used for FISH probes and dsRNA. Related to all figures.

Figure S1

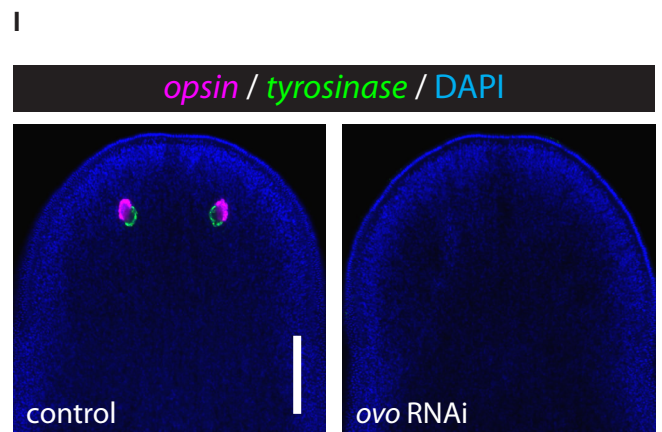
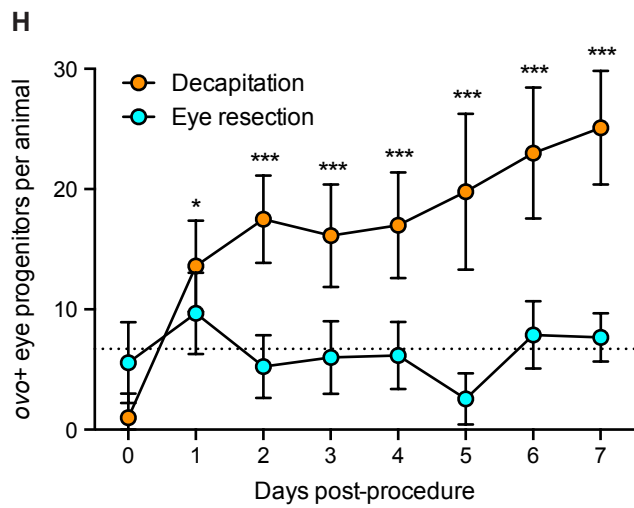
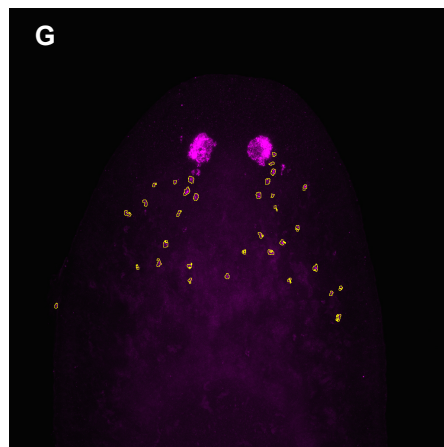
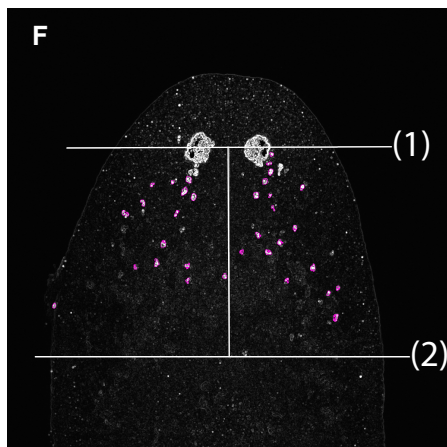
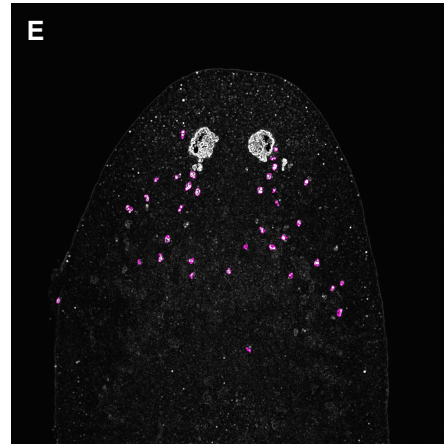
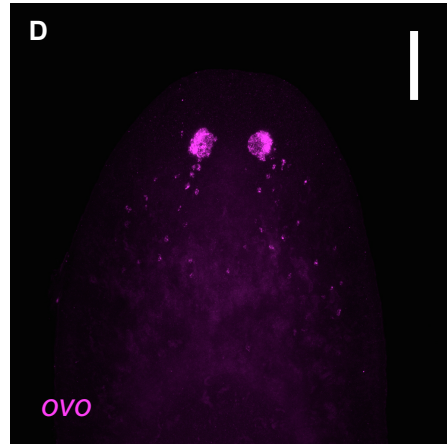
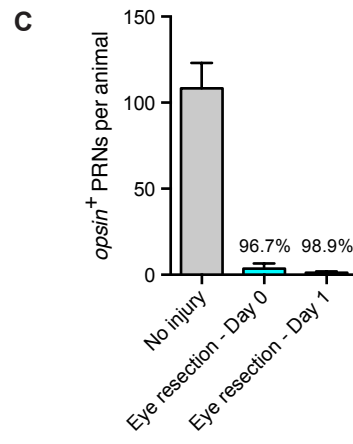
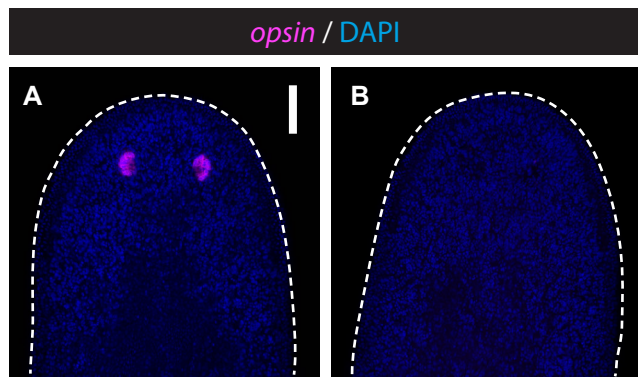


Figure S1. Eye resection controls and semi-automated eye progenitor counting procedure and results. Related to Figures 1 and 2

(A and B) FISH for *opsin* with DAPI labeling in uninjured animals (A) and eye-resected animals (B) 1 day post-surgery demonstrates PRN removal. Dashed white line indicates animal boundary. Scale bar, 100 μm .

(C) PRNs per animal in uninjured and eye-resected animals, 0 and 1 day post-surgery. $n \geq 6$ animals per condition. Data represented as mean \pm SD. Percentages indicate % PRN removal (mean number of PRNs per animal after resection / mean number of PRNs per animal in intact animals \times 100). Day 0 and Day 1 eye resection data are also shown in Figure S5 regeneration timecourse.

(D-G) Semi-automated progenitor counting procedure. (D) Representative maximum intensity projection from z-stack of FISH for *ovo* in decapitated animal seven days post-surgery. Scale bar, 100 μm . (E) Appearance of image after processing algorithm. Computer-identified eye progenitors are outlined in magenta. (F) Lines indicate area of progenitor counting, defined as the area between a line running through the eyes (1) and a parallel line 300 μm posterior to the first (2). Events touching the line are counted, events completely outside lines or completely inside eye are not counted.

(G) All counted progenitor outlines (yellow) overlaid on original maximum intensity projection.

(H) *ovo*⁺ eye progenitor numbers 0 to 7 days post-surgery, as quantified by semi-automated progenitor counting. Data represented as mean \pm SD. Dotted line represents mean of uninjured animals on Day 0. Decapitation but not eye resection results in significantly elevated eye progenitor numbers in comparison to uninjured controls. Statistical significance assessed with respect to uninjured animals by one-way ANOVA (* $p < 0.05$, *** $p < 0.001$).

(I) FISH for *opsin* and *tyrosinase* with DAPI labeling in eye-resected animals 1 week post-surgery under control RNAi and *ovo* RNAi conditions. Control RNAi animals regenerated normal eyes containing *tyrosinase*⁺ pigmented optic cup cells and *opsin*⁺ PRNs (10 of 10 animals). *ovo* RNAi animals failed to regenerate eyes (10 of 10 animals had ≤ 3 PRNs, 6 of 10 had 0 PRNs). Scale bar, 200 μm .

Figure S2

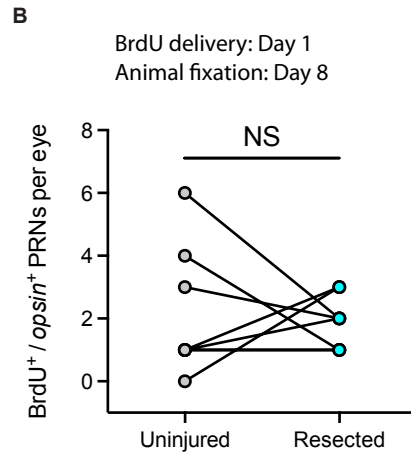
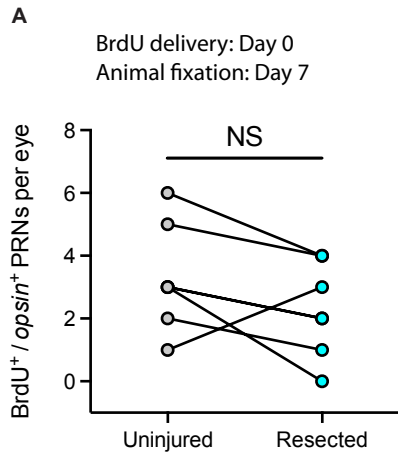


Figure S2. Additional single eye resection BrdU incorporation experiments. Related to Figure 3.
(A and B) BrdU/*opsin* double-positive PRNs per eye after single eye resection. (A) BrdU delivery Day 0, animal fixation Day 7. $n=7$ animals. (B) BrdU delivery Day 1, animal fixation Day 8. $n=8$ animals. Statistical significance assessed by paired Student's *t*-tests (NS, not significant).

Figure S3

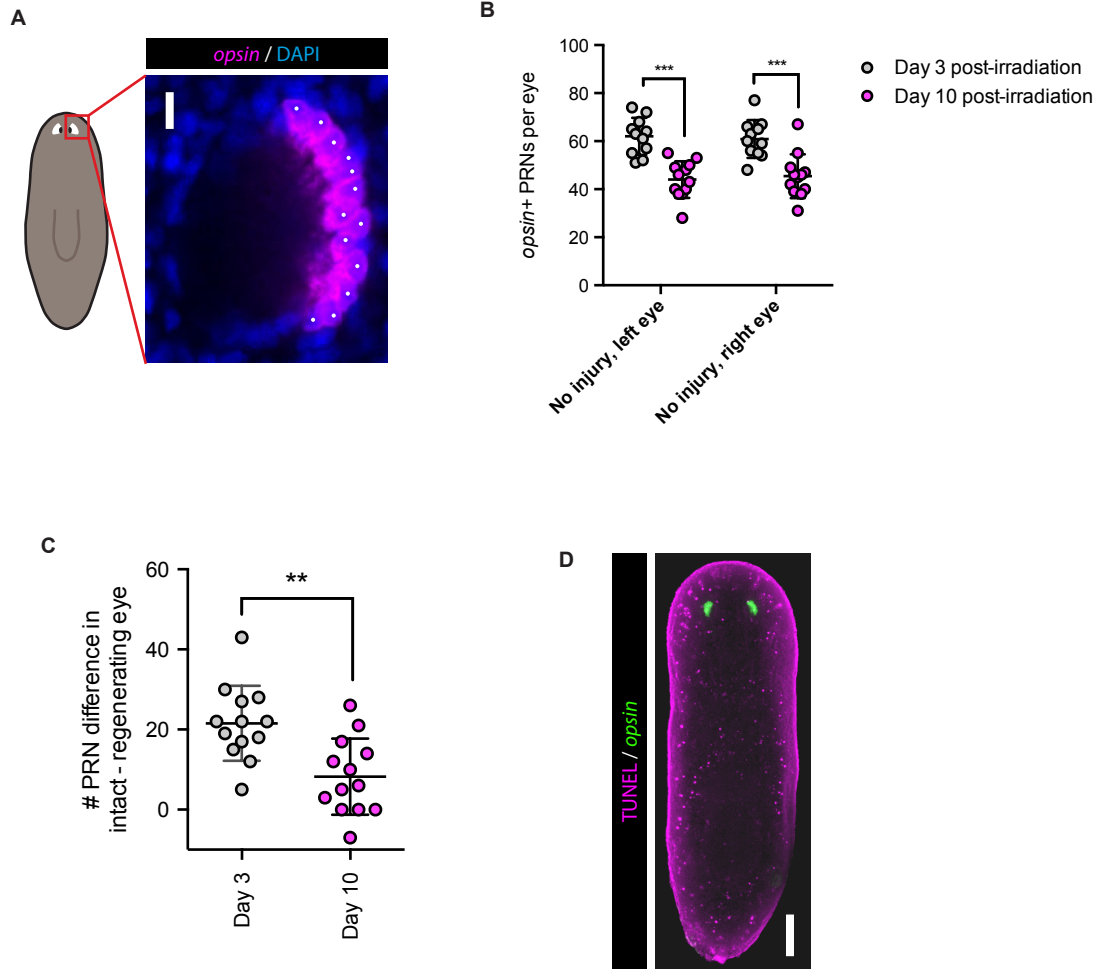


Figure S3. Cell loss controls and combined TUNEL and FISH for *opsin*. Related to Figure 4.

(A) Example of PRN counting in a single eye. FISH for *opsin* with DAPI labeling. Single confocal optical section, showing individual PRNs marked with white spots. All PRN counting was performed blind to condition. Scale bar, 10 μ m.

(B) PRNs per eye, 3 and 10 days post-irradiation in uninjured animals. Data represented as mean \pm SD. Dots represent PRN counts for individual eyes. Statistical significance assessed by Student's *t* test (***p*<0.001).

(C) Intra-animal difference in PRN number (uninjured – regenerating), decreases from Day 3 to Day 10 post-irradiation. Data represented as mean \pm SD. Dots represent differences from individual animals. Statistical significance assessed by paired Student's *t* test (***p*<0.01).

(D) Combined TUNEL and FISH for *opsin*. Maximum intensity projection. Scale bar, 100 μ m.

Figure S4

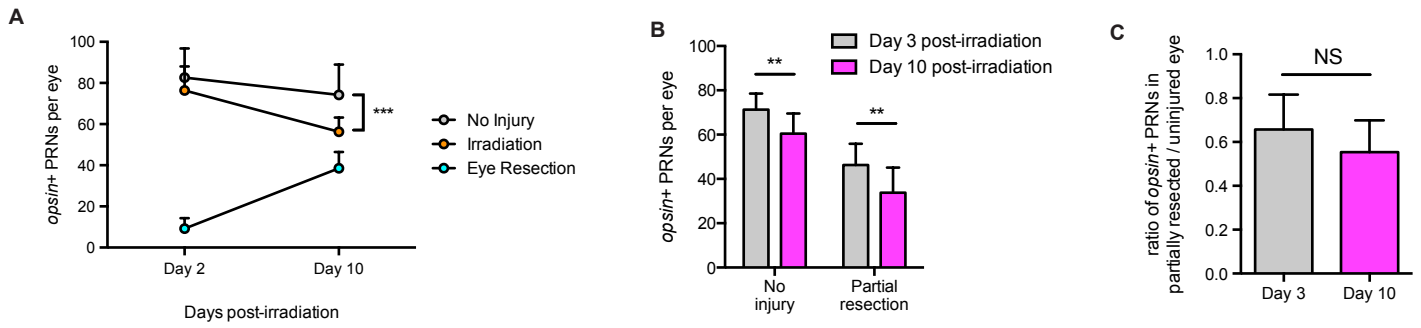


Figure S4. Dynamics of eye growth and de-growth are consistent with a passive model for tissue-specific eye regeneration. Related to Figures 4 and 5.

(A) PRNs per eye Day 2 and Day 10 after indicated manipulation. Data represented as mean \pm SD.

Significance assessed by Student's *t*-test (** $p < 0.001$). $n \geq 10$ animals per condition.

(B and C) Uninjured and partially resected eyes undergo cell loss at similar rates. (B) PRNs per eye Day 3 and Day 10 post-irradiation for indicated surgeries. (C) Intra-animal ratio of PRNs in regenerating/intact eyes remained constant from Day 3 to Day 10 post-irradiation. Data represented as mean \pm SD.

Significance assessed by Student's *t*-test (** $p < 0.01$); NS, not significant. $n = 12$ animals per timepoint.

Figure S5

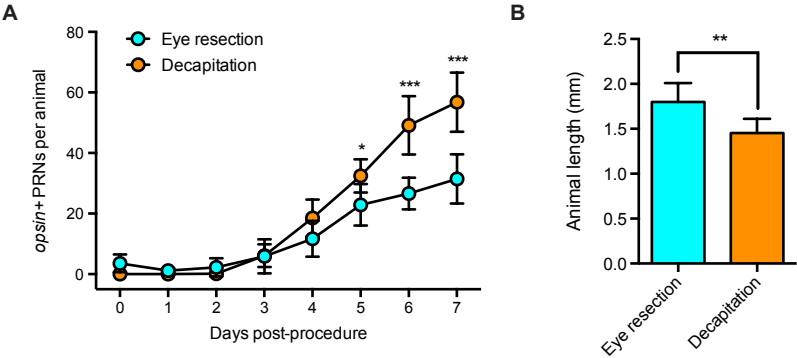


Figure S5. Eye-resected animals regenerate eyes more slowly than decapitated animals. Related to Figure 5.

(A) PRN regeneration timecourse following decapitation or eye resection. PRNs per animal Day 0 to Day 7 post-procedure are shown. Decapitated animals have a significantly greater number of PRNs than eye-resected animals at 5, 6 and 7 days post-procedure. Animals are same as used for eye progenitor counting in Figure 2D. Day 0 and Day 1 eye resection data is also shown in Figure S1C. Data represented as mean \pm SD. Statistical significance assessed by Student's *t*-test (* $p < 0.05$, *** $p < 0.001$). $n \geq 4$ animals per condition.

(B) Animal length seven days post-surgery. Decapitated animals are significantly shorter than eye-resected animals. Data represented as mean \pm SD. Statistical significance assessed by Student's *t*-test (** $p < 0.01$). $n \geq 9$ animals per condition.

Figure S6

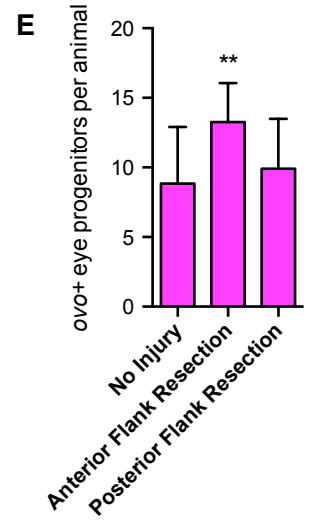
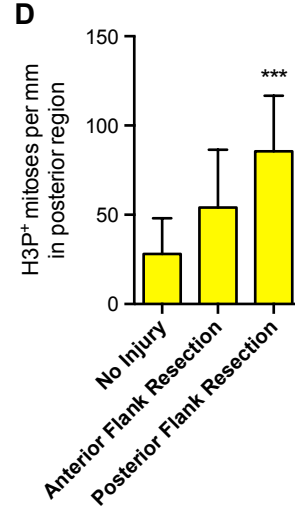
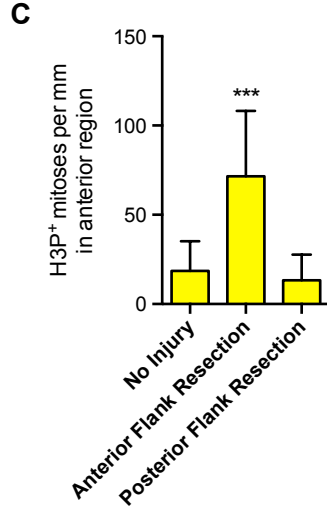
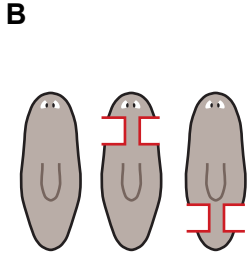
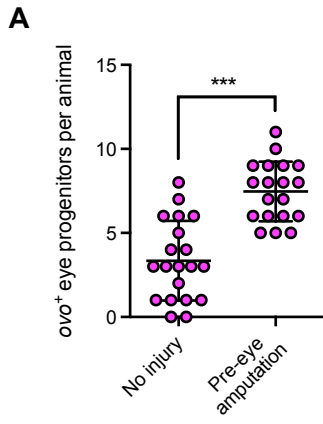


Figure S6. Eye progenitor amplification is associated with wounds that induce proliferation in the location of eye progenitor specification. Related to Figures 6 and 7.

(A) Independent experiment determining the effect of pre-eye amputation on eye progenitor numbers. *ovo*⁺ eye progenitors per animal 4 days after no injury and pre-eye amputation, as depicted in Figure 6G. Pre-eye amputation induces significant increase in eye progenitor numbers. Data represented as mean ± SD. Dots represent values from individual animals. Statistical significance assessed by Student's *t*-test (***p*<0.001).

(B) Cartoon depiction of uninjured animal (left), anterior flank resection (center), and posterior flank resection (right).

(C and D) H3P⁺ cells per mm in anterior (C) and posterior (D) regions 48 hours after surgeries indicated in (B). Data from (C) is also displayed in Figure 7D. Data represented as mean ± SD. Statistical significance assessed with respect to uninjured animals by one-way ANOVA (***p*<0.001). *n*≥9 animals per condition.

(E) *ovo*⁺ eye progenitors per animal 4 days after surgeries depicted in (B). Data represented as mean ± SD. Significance assessed with respect to uninjured animals by one-way ANOVA (***p*<0.01). *n*≥11 animals per condition.

Figure S7

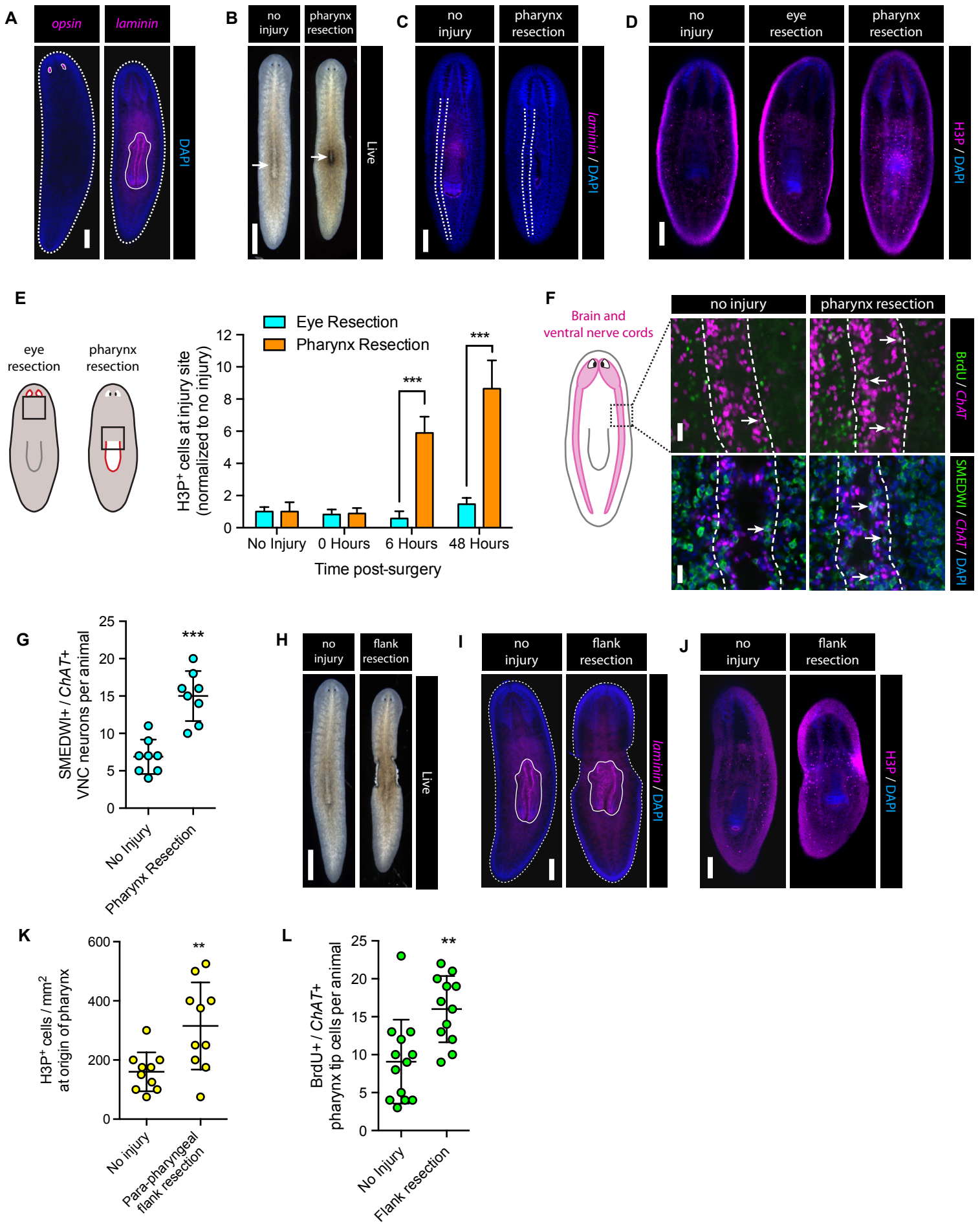


Figure S7. Increased progenitor incorporation into the ventral nerve cords and pharynx does not require specific tissue removal. Related to Figure 7.

- (A) FISH for *opsin* or *laminin* with DAPI labeling. *laminin* marks pharynx tissue. Dashed lines indicate animal boundaries, solid lines indicate borders of PRNs or pharynx. Scale bar, 200 μm . The pharynx is much larger than the eyes.
- (B) Live images of the same animal immediately before (left) and after (right) dorsal surgical pharynx resection. Arrow indicates location of pharynx (left) or location of dorsal incision through which pharynx was excised (right). Scale bar, 1 mm.
- (C) FISH for *laminin* with DAPI labeling after no injury and dorsal surgical pharynx resection. Dashed white lines indicate left ventral nerve cord (VNC). Scale bar, 200 μm . Surgery removes pharynx and leaves VNCs continuous and intact.
- (D) IF for H3P with DAPI labeling in uninjured, eye-resected and pharynx-resected animals 48 hours post-surgery. Scale bar, 200 μm . Pharynx-resected but not eye-resected animals display increased mitotic activity near the site of tissue removal.
- (E) Cartoons depict surgeries (red lines) and location of quantification (black boxes) for eye- and pharynx-resected animals. Graph indicates mitotic density at indicated times post-surgery, normalized to mean of uninjured animals. Pharynx but not eye resection induces sustained local neoblast proliferation.
- (F) IF for BrdU with FISH for *ChAT* (top insets) and IF for SMEDWI with FISH for *ChAT* and DAPI labeling (bottom insets) after no injury or pharynx resection. Dashed white lines indicate VNC boundaries. Arrows indicate BrdU⁺/*ChAT*⁺ or SMEDWI⁺/*ChAT*⁺ VNC cells. Scale bars, 20 μm .
- (G) SMEDWI⁺/*ChAT*⁺ VNC neurons per animal 4 days after no injury or pharynx resection. Quantification performed in VNC just anterior to pharynx. Data represented as mean \pm SD. Dots represent values from individual animals. Significance assessed by Student's *t*-test (***p*<0.001).
- (H) Live images of the same animal immediately before (left) and after (right) para-pharyngeal flank resection. Scale bar, 1 mm.
- (I) FISH for *laminin* with DAPI labeling in animals fixed immediately after no injury or para-pharyngeal flank resection. Dashed white lines indicate animal boundaries, solid white lines outline pharynges. Scale bar, 200 μm . Para-pharyngeal flank resection does not remove pharynx tissue.
- (J) IF for H3P with DAPI labeling 48 hours after no injury or para-pharyngeal flank resection. Scale bar, 200 μm . Flank resection increases mitotic activity near the pharynx.
- (K) Mitotic density near pharynx 48 hours after no injury or para-pharyngeal flank resection. Data represented as mean \pm SD. Dots represent values from individual animals. Significance assessed by Student's *t*-test (***p*<0.01).
- (L) BrdU⁺/*ChAT*⁺ pharynx tip cells per animal after no injury or para-pharyngeal flank resection. BrdU delivery Day -1, fixation Day 4 with respect to surgery. Data represented as mean \pm SD. Dots represent values from individual animals. Significance assessed by Student's *t*-test (***p*<0.01).

Supplemental Tables

Table S1. Animal numbers for all experiments. Related to all figures.

The table indicates the number of animals used for all experiments involving quantification, with corresponding figure number and condition.

Table S2. Sequences used for FISH probes and dsRNA. Related to all figures.

The table indicates sequences used for FISH probes and dsRNA, with references.